Biophysical Chemistry 151 (2010) 61–70

Contents lists available at ScienceDirect

Biophysical Chemistry

journal homepage: http://www.elsevier.com/locate/biophyschem

Sidechain conformational dependence of hydrogen exchange in model peptides

Janet S. Anderson [a], Griselda Hernández [b], David M. LeMaster [b,*]

[a] Department of Chemistry, Union College, Schenectady, NY 12308, USA
[b] Wadsworth Center, New York State Department of Health and Department of Biomedical Sciences, School of Public Health, University at Albany — SUNY, Empire State Plaza, Albany, NY 12201, USA

ARTICLE INFO

Article history:
Received 16 March 2010
Received in revised form 10 May 2010
Accepted 12 May 2010
Available online 19 May 2010

Keywords:
Protein sidechain
Hydrogen exchange
Amide acidity
Peptide conformation
Continuum electrostatics
Dielectric shielding

ABSTRACT

Peptide hydrogens that are exposed to solvent in protein X-ray structures exhibit a billion-fold range in hydroxide-catalyzed exchange rates, and these rates have previously been shown to be predictable by continuum dielectric methods to within a factor of 7, based on single protein conformations. When using a protein coil library to model the Boltzmann-weighted conformational distribution for the various N-acetyl-[X-Ala]-N-methylamides and N-acetyl-[Ala-Y]-N-methylamides, the acidity of the central amide in the individual conformers of each peptide spans nearly a million-fold range. Nevertheless, population averaging of these conformer acidities predicts the standard sidechain-dependent hydrogen exchange correction factors for nonpolar model peptides to within a factor of 30% ($10^{0.11}$) with a correlation coefficient $r = 0.91$. Comparison with the analogous continuum dielectric calculations for the other N-acetyl-[X-Y]-N-methylamides indicates that deviations from the isolated residue hypothesis of classical polymer theory predict appreciable errors in the exchange rates for conformationally disordered peptides when the standard sidechain-dependent hydrogen exchange rate correction factors are assumed to be independently additive. Although electronic polarizability generally dominates the dielectric shielding for the ~10 ps lifetime of peptide ionization, evidence is presented for modest contributions from rapid intrarotamer conformational reorganization of Asn and Gln sidechains.

1. Introduction

The early studies of Linderstrøm-Lang and colleagues reported that the amides of the protein backbone exhibit a wide range of hydrogen exchange rates [1,2]. These researchers interpreted this large spread in rates as resulting from transient solvent exposure for the amides that are normally buried within the native state structure of the protein, thus providing the first direct experimental demonstration of protein conformational flexibility. Reflecting the fact that their studies were carried out before the first protein X-ray structure was reported, Linderstrøm-Lang and colleagues proposed that the conformational flexibility within the folded protein structure can be estimated through comparison of the exchange rates from the protein amides to those of simple model peptides [3,4]. During the subsequent fifty years, protein hydrogen exchange has routinely been interpreted as a passive monitor of solvent accessibility. Under most common experimental exchange conditions, an equilibrium is established between the conformational ground state and the transient exchange-competent conformation(s) before the hydrogen exchange reaction occurs. Under the assumption that exposure to solvent implies exchange reaction rates equivalent to those of simple model peptides, the ratio of the observed exchange rate to that of a corresponding model peptide defines a residue-specific free energy (i.e., $\Delta G = -RT\ln(k_{ex}/k_{pep})$) for the conformational transition(s) that give rise to solvent exposure of that amide hydrogen [5].

The inadequacy of a simple solvent accessibility interpretation is demonstrated by the billion-fold range in hydroxide-catalyzed exchange rates exhibited by protein amide hydrogens that are well exposed to solvent in high resolution X-ray structures [6,7]. Standard continuum dielectric methods have been proven exceedingly useful for interpreting the electrostatic interactions underlying this wide range of protein hydrogen exchange rates. The electrostatic free energy of a Born ion imbedded in a high dielectric solvent is inversely proportional to the internal dielectric value [8]. Applying this paradigm to a protein for which multiple ionizations can be predicted simultaneously, the electrostatic model of atom-centered fixed partial charges and a uniform volume polarizability might be expected to provide a basis for not only estimating the optimal effective internal dielectric value but also for assessing the robustness of the uniform dielectric shielding assumption. It is well known that applying continuum dielectric methods to protein sidechain ionizations generally does not yield predictions that are consistent with a well-determined uniform internal dielectric value [9–14]. Protein conformational reorganization contributes strongly to the dielectric shielding of these sidechain ions [15], giving rise to heterogeneity in the spatial attenuation of electrostatic interactions.

* Corresponding author. Tel.: +1 518 474 6396; fax: +1 518 473 2900.
E-mail address: lemaster@wadsworth.org (D.M. LeMaster).

0301-4622/$ – see front matter © 2010 Elsevier B.V. All rights reserved.
doi:10.1016/j.bpc.2010.05.006

As long discussed in electron transfer theory [16], dielectric shielding is frequency dependent. The lifetime of a transient charge state determines the range of conformational motions that can give rise to effective dielectric shielding. In marked contrast to the μs–ms lifetimes of the sidechain charge states near neutral pH, the peptide anion intermediates formed during the hydrogen exchange reaction have lifetimes of ~10 ps. Since only the quite limited protein conformational transitions that occur within this brief lifetime can significantly contribute to the dielectric shielding of the peptide anion, the effective internal dielectric value for protein hydrogen exchange is dominated by electronic polarizability [6,7,17]. Amides have been experimentally demonstrated [18,19] to act as normal Eigen acids [20], so that the thermodynamic acidity of an amide directly predicts its kinetic acidity as monitored by the hydrogen exchange reaction.

Application of Poisson–Boltzmann continuum dielectric methods to the high resolution X-ray structures of four model proteins has yielded values of the electrostatic potential at 56 solvent-exposed backbone amide sites which predict the billion-fold variation in exchange rates to within an rmsd of 7 [7]. The slope of correlation between predicted and observed hydrogen exchange rates yielded an optimal internal dielectric value of 3, closely approximating the predicted electronic polarizability contribution when the packing density of the protein interior is considered [21]. The slope of the correlation between the predicted and observed hydrogen exchange rates for these four proteins varies inversely with the assumed internal dielectric value [7], while the reasonably modest errors in the hydrogen exchange rate predictions argue strongly against the presence of large differences in the effective internal dielectric shielding at the various backbone amide sites.

Such calculations based on a single protein conformation oversimplify the problem, since it is the full range of energetically accessible conformations that determines the observed hydrogen exchange kinetics in solution. Given that efforts to accurately model the native state Boltzmann conformational distribution have been most actively pursued for ubiquitin, we have demonstrated [22] that two such model ubiquitin ensembles, constrained to fit NMR relaxation [23] and NMR residual dipolar coupling [24] data, yield hydrogen exchange rate predictions for 16 highly exposed amides that match the nearly million-fold range in ubiquitin experimental values to within an rmsd of 3 with a correlation coefficient $r = 0.94$. In terms of the number of sites predicted, the rmsd of the pK prediction errors, and the statistical significance of these amide acidity predictions, these results compare quite favorably with the protein sidechain pK prediction studies published to date, based on either continuum dielectric methods [9–14] or other modeling paradigms [25–32]. The utility of continuum dielectric methods is not limited to prediction of exchange kinetics at the highly exposed protein amide sites. Poisson–Boltzmann analysis of the more rarely exposed amide sites in these two NMR-restrained model ubiquitin ensembles [23,24] demonstrated that hydrogen exchange provides a powerful experimental basis for distinguishing whether or not a given model ensemble is consistent with a proper Boltzmann-weighted conformational distribution [22].

Predicting the experimental sidechain-dependent differential exchange rates for conformationally unstructured peptides presents a rather stringent challenge. Although early studies argued that the differences in exchange rates among various simple model peptides arise from chemical induction effects [18,33], more recent electrostatic calculations have indicated that amide hydrogen exchange rates are strongly dependent upon the relative orientation of the adjacent peptide groups [34,35]. Reorientation of these peptide groups gives rise to million-fold variations in the predicted amide acidities for conformations observed in high resolution protein X-ray structures [36]. Yet when averaged over the Boltzmann-weighted conformational distribution during an experimental measurement, substitution of different sidechains into simple model peptides produces less than 3-fold changes in exchange rate for most residue types [37]. As a result, a compelling correlation between predicted and observed sidechain-dependent hydrogen exchange rate differences for conformationally unstructured peptides requires substantially more accurate predictions than have yet been demonstrated in protein studies.

Applying continuum dielectric methods with an internal dielectric value of 4, McCammon and colleagues [34] found that the log correction factors for the sidechains preceding the exchanging amide could be predicted with an rmsd of 0.17 for the set of experimental hydroxide-catalyzed exchange rate constant values ($\Delta\log k_{OH^-}$). For the larger range of differential log exchange rates that arise from altering the intraresidue sidechain, those authors obtained an appreciably worse fit with an rmsd of 0.38, comparable to the spread within the set of experimental log rate values. More recently, Avbelj and Baldwin [35] presented a Poisson–Boltzmann analysis of the steric contributions to the sidechain dependence of hydrogen exchange in which the peptide N, H, C and O atoms were assigned partial charges from the PARSE [38] parameter set, with all other atomic charges set to zero. For the various sidechain types, the predicted differences in electrostatic free energies, relative to the alanine reference, were roughly twice as large when the residue bearing the exchanging amide was placed in a polyproline II ($\phi,\psi = -70°, 150°$) conformation as compared to when it was placed in an extended ($\phi,\psi = -120°, 120°$) conformation.

In these earlier electrostatic modeling studies of the sidechain-dependent exchange rates, the problem was simplified by assuming the same backbone conformation for each residue type. This assumption suppresses the largest source of variation among the individual amide acidity calculations. However, as a result, insight into the impact of the different sidechain types upon the conformational distribution of the backbone is lost. A more complete analysis of the model peptide exchange rates requires an accurate representation of the Boltzmann-weighted distribution of conformations. Unfortunately, there remains a wide disparity among the current predictions of the relative populations of helical, extended, polyproline II and other local backbone conformations for simple model peptides [39–44].

Following our recent study of the backbone conformational dependence of peptide hydrogen exchange [36], the present analysis has utilized the Protein Coil Library of Rose and colleagues [45] as a model for the Boltzmann-weighted distribution of the unstructured state. In this structural library, protein segments lying outside of regular secondary structures were identified from high resolution X-ray analysis. From the atomic coordinates of these segments, model N-acetyl-[X-Ala]-N-methylamides and N-acetyl-[Ala-Y]-N-methylamides were constructed and then used to predict the experimental sidechain correction factors for hydrogen exchange [37], while the other N-acetyl-[X-Y]-N-methylamides are subsequently used to assess whether anticipated deviations from additivity for these correction factors [35,46] are observed.

2. Computational methods

2.1. Crystallographic dipeptide conformer modeling

The 17,422 protein segments selected from X-ray structures having at least 1.6 Å resolution and R values of 0.25 or better in the Protein Coil Library of Rose and colleagues [45] were divided into dipeptide segments. The terminal residues of each segment were excluded so as to further reduce residual conformational bias that could arise from the presence of adjacent regular secondary structure [47]. As noted in our previous analysis of the backbone conformational dependence of amide acidity [36], peptides with significantly distorted geometry can give rise to anomalous electrostatic free energy predictions. Every backbone bond length and bond angle for each dipeptide segment was compared against the standard

values, as given by the Procheck [48] program. Each dipeptide segment having any backbone bond length or bond angle that deviates by more than 3 σ from the standard value was excluded from the subsequent analysis. Approximately 5% of the dipeptide segments were removed by this criterion. The Reduce program [49] was used to add hydrogens to the heavy atoms in the backbone segment that extends between the C^{α} atoms on either side of the selected dipeptide, yielding N-acetyl-[X-Y]-N-methylamides. Given the comparatively modest fraction of neutral forms for the Asp, Glu, Lys and Arg sidechains anticipated to be represented in the Protein Coil Library, all such conformers were assumed to be in the charged state. Analysis of the histidine residues was not pursued due in part to the ambiguities in both the charge of the sidechain and the tautomeric state of the neutral imidazole form in the structural library.

2.2. Calculation of peptide conformer acidity

Nonlinear Poisson–Boltzmann calculations were carried out using the DelPhi algorithm [50], with CHARMM22 atomic charge and atomic radius parameters [51], modified to include density functional theory-derived atomic charges for the peptide anion [7]. A 0.25 Å grid spacing was used with a 50% filling factor and an ionic radius of 2.0 Å. The external dielectric value was set to 78.5 and an ionic strength of 0.15 M was used, except where noted otherwise. To facilitate comparisons between the various model peptide structures, electrostatic calculations were carried out for each N-acetyl-[X-Y]-N-methylamide peptide with an N-methylacetamide molecule added to the lattice grid for internal referencing of the differential electrostatic potential. The N-methylacetamide was positioned such that the distance between the N-methylacetamide nitrogen and the nearest formal charge was at least 16 Å and no intermolecular atomic distance was less than 8 Å. For each peptide conformer, three calculations were carried out: the peptide anion in the presence of the neutral N-methylacetamide; the neutral peptide in the presence of the N-methylacetamide anion; and the neutral peptide in the presence of the neutral N-methylacetamide which serves as the common reference state. The calculated difference in electrostatic free energy for transferring a proton from a neutral peptide conformer to an N-methylacetamide anion is related to the difference in acidity by their mutual relationship to the difference in the electrostatic potential at that site times the elementary charge ($\Delta G_{elec}(kT) = e\Delta V = \Delta pK * \ln[10]$). To assess the errors arising from the positioning of molecules in the lattice grid summation, the difference in electrostatic free energy predicted between the neutral and anionic N-methylacetamide molecules for each of the peptide conformer calculations was found to be consistent with our previously reported [36] average grid error of 0.036 log units in the relative pK values.

2.3. Hydrogen exchange prediction from population averaging of peptide conformer acidities

As the amide hydrogen has been shown [18,19] to exchange as a normal Eigen acid [20], the known acidity of water (pK_a of 15.7 at 25 °C) and the diffusion-limited reactivity with hydroxide ion ($2\times10^{10}\ M^{-1}\ s^{-1}$ at 25 °C [18,19]) imply a hydroxide-catalyzed hydrogen exchange rate constant of $1.0\ M^{-1}\ s^{-1}$ for an amide with a pK of 26. The electrostatic free energy calculations predict the ΔpK values among the various peptide conformers. Under the assumption that chemical induction effects are negligible, the experimental exchange rate data on N-acetyl-[Ala-Ala-Ala]-N-methylamide was used to place these ΔpK values on an absolute scale. The hydroxide-catalyzed H → D log exchange rate constant for the central amide of N-acetyl-[Ala-Ala-Ala]-N-methylamide at 20 °C has been reported to be $10.36\ M^{-1}\ min^{-1}$ [37]. Correcting for temperature [37] and isotope effect [52], the log k_{OH-} value of $8.69\ M^{-1}\ s^{-1}$ was used to calibrate the Poisson–Boltzmann predicted acidity for the Ala-Ala peptide ensemble. By thus establishing the difference in pK between water and the central amide from each peptide conformer, the fraction of forward-reacting exchange encounters $K_i/(K_i+1)$ is determined, where K_i is the equilibrium constant for the transfer of a proton from the amide to a hydroxide ion [20]. As indicated in the following section, most peptide conformers have amide acidities that are appreciably less than that of water so that only a modest correction for the diffusion-limited reaction applies. The exchange reactivities for the individual conformers were then averaged over the ensemble population to derive the predicted hydrogen exchange rate.

3. Results and discussion

3.1. Continuum dielectric predictions for the kinetic acidity of peptides

As earlier predicted by Eigen [20], amides have been experimentally demonstrated [18,19] to act as normal Eigen acids such that the reaction rate with hydroxide ion is attenuated from the diffusion limit by the fraction of forward-reacting encounters $K_i/(K_i+1)$, where K_i is the equilibrium constant for the transfer of a proton from the amide to an hydroxide ion. Although a direct measurement of how rapidly the peptide anion is quenched by a neutral water molecule has not been reported, NMR relaxation studies indicate that the residence lifetime of an hydroxide ion in water is ~5 ps [53], and lifetimes near 10 ps have commonly been observed for photoactivated strong acids [54,55]. Noting that the dominant phase of the Debye dielectric relaxation profile for water has a time constant of 8 ps at 25 °C [56], it has been argued that the dynamics of water reorientation are limiting in these fast proton transfer reactions [54,55]. By analogy, the lifetime of the peptide anion intermediate is likewise anticipated to be ~10 ps [6,7,17].

Only a limited set of protein conformational reorganization transitions can occur rapidly enough to substantially contribute to the dielectric shielding of such a short-lived charge state. As a result, electronic polarizability is anticipated to dominate the observed shielding response for amide hydrogen exchange [6,7,17]. The electronic polarizability of the protein interior has often been modeled by assuming an internal dielectric value of 2.0 that is derived from refractive index measurements on typical organic liquids which monitor the dielectric response at optical frequencies ($\sim10^{15}\ s^{-1}$). However, noting that the density within the protein interior is 30–40% higher than that of analogous small molecule liquids [57,58], Mertz and Krishtalik [21] have argued that the average contribution of electronic polarizability implies a dielectric shielding value of at least 2.5 for protein molecules.

Given the high dielectric value of the aqueous solvent phase, the generalized-Born formula for an ion of charge Q and radius R predicts that the electrostatic free energy is essentially inversely proportional to the value of the internal dielectric [8]:

$$\Delta G_{elec} = -(1/\varepsilon_{int} - 1/\varepsilon_{ext})Q^2/2R.$$

Poisson–Boltzmann calculations on a set of four globular proteins have demonstrated that the anticipated inverse proportionality between predicted peptide acidities and the internal dielectric value is well preserved for these more complex geometries [7]. As a result, the slope of the correlation between the experimental and predicted peptide acidities provides a sensitive monitor of the optimal effective internal dielectric value, while the precision of that correlation yields an upper bound to the errors arising from the assumed spatial uniformity of the internal dielectric. The optimal internal dielectric value of 3 derived from the analysis of the hydrogen exchange for the static solvent-exposed amides in these same four globular proteins [6,7] closely approximates the value estimated by Mertz and Krishtalik [21] and strongly vindicates the prediction that electronic polarizability dominates the dielectric shielding of protein peptide

anions. Given the higher degree of conformational flexibility within simple model peptides, the correlation between the experimental and predicted peptide acidities should provide a sensitive test for the relative contribution of conformational dynamics in high frequency dielectric shielding.

Following the earlier peptide exchange analyses of McCammon and colleagues [34] and Avbelj and Baldwin [35], our previous analysis of the backbone conformational dependence of peptide acidity [36] assumed that the excess negative charge of the peptide anion resides exclusively on the nitrogen. That assumption conflicts with the long-standing tradition of referring to the product formed by deprotonation of an amide as an imidate anion. However, in contrast to predictions from early valence bond theory studies, there are no experimental results or high level quantum mechanical calculations which support the interpretation that a dominant fraction of the excess negative charge for a secondary alkyl amide anion shifts to the oxygen atom [59]. Recently, we reported [7] B3LYP [60] density functional theory calculations at the aug-cc-pVTZ basis set level on the neutral and anionic states of N-methylacetamide. These calculations predicted an electron charge distribution for the peptide anion that assigns a 3-fold higher excess charge density for the nitrogen atom than for the oxygen atom. The DFT-derived peptide anion charge distribution provided somewhat better protein hydrogen exchange predictions than did an assignment of the excess charge to the nitrogen. However, assignment of the excess negative charge to the oxygen, so as to generate the imidate form, yielded markedly poorer predictions than for either of the other two peptide anion charge distributions [7].

As compared to the conformational complexity of the protein native state, it might be anticipated that accurate prediction of the Boltzmann-weighted conformational distribution for simple model peptides should be relatively straightforward. In fact, even the basic question of the relative fraction of extended vs. α conformational populations in model peptides remains an actively debated issue [39–41]. Current implementations of classical molecular dynamics simulations [42,43], as well as density functional theory-based modeling [44], continue to yield disparate predictions for the backbone conformational distributions of simple model peptides.

As typified by recent studies of Rose and colleagues [45], numerous protein coil conformational libraries have been derived from high resolution protein X-ray structures by deleting the residues involved in regular secondary structural elements. Generally implicit in the application of these coil libraries is the assumption that the other forms of long range interactions which are present in the protein crystal structure do not systematically shift the average conformational distribution of the individual residue types away from that which occurs for conformationally disordered polypeptides. Given the success with which electrostatic analysis of hydrogen exchange from the native state of ubiquitin can distinguish the consistency of a given model conformational ensemble with the correct Boltzmann distribution, it was anticipated that the analogous study of hydrogen exchange in model peptides based on electrostatic analysis of a protein coil library distribution might provide further insight into the utility of these libraries as representations of the disordered conformational state.

In the absence of chemical induction effects, the difference in acidity between two solvent-exposed peptides depends upon the difference in electrostatic free energy for the two corresponding peptide anions. In the present study, along with each N-acetyl-[X-Y]-N-methylamide conformer derived from the Protein Coil Library of Rose and colleagues [45], a N-methylacetamide molecule is placed on the lattice grid used in the finite difference calculation of the DelPhi [50] Poisson–Boltzmann algorithm. The free energy of transfer for a proton from the N-acetyl-[X-Y]-N-methylamide anion to the N-methylacetamide anion is proportional to the ΔpK for these two amide nitrogens ($\Delta pK = \Delta G_{elec}/(\ln[10])$). As noted in our previous analysis of the backbone conformational dependence of model peptide exchange [36], the average error for these differential pK calculations arising from variation in the placement of molecules onto the lattice grid was estimated to be 0.036 pH units.

3.2. Ensemble-averaged amide hydrogen exchange predictions for nonpolar sidechains

Experimentally measured hydroxide-catalyzed amide exchange rates for conformationally unstructured alanine peptides are essentially unaffected by the intraresidue substitution of a methionine sidechain, while substitution of a phenylalanine, tyrosine or tryptophan sidechain decreases the exchange rate by approximately two-fold [37]. A significantly larger (~5-fold) attenuation of the exchange rates results from substituting any of the branched sidechains from valine, leucine or isoleucine. A similar pattern is obtained when these sidechain substitutions are introduced into the residue preceding the site of amide exchange, although the magnitude of the variations in exchange rates is approximately 4-fold smaller.

To assess the degree to which these nonpolar sidechain effects on hydrogen exchange can be predicted, we carried out continuum dielectric calculations on implicitly solvated N-acetyl-[X-Ala]-N-methylamide and N-acetyl-[Ala-Y]-N-methylamide conformers derived from the Protein Coil Library [45], using the DelPhi program [50]. As illustrated in Fig. 1, amide acidities were calculated for 458 N-acetyl-[Ala-Val]-N-methylamide conformers. A nearly million-fold range in conformer acidities was observed, similar in magnitude to the range previously reported for the conformers of alanine and glycine-containing peptides derived from the same library [36]. The ΔpK values obtained from the Poisson–Boltzmann calculations were placed on a pK scale, making use of the known acidity of water (pK_a of 15.7 at 25 °C), the diffusion-limited reactivity of amides with hydroxide ion ($2\times10^{10}\ M^{-1}\ s^{-1}$ at 25 °C [18,19]), and the experimental hydroxide-catalyzed rate constant for the central peptide of N-acetyl-[Ala-Ala-Ala]-N-methylamide [37].

The other nonpolar N-acetyl-[X-Ala]-N-methylamide and N-acetyl-[Ala-Y]-N-methylamide conformers predict a similar range of conformer acidities, suggesting that the relative orientation of the adjacent peptide groups provides the dominant contribution to the amide acidities. In turn, it is the distribution of the sidechain conformations for the more acidic mainchain conformations that will primarily determine the observed sidechain-dependent differential exchange rates. The degree to which the backbone geometry

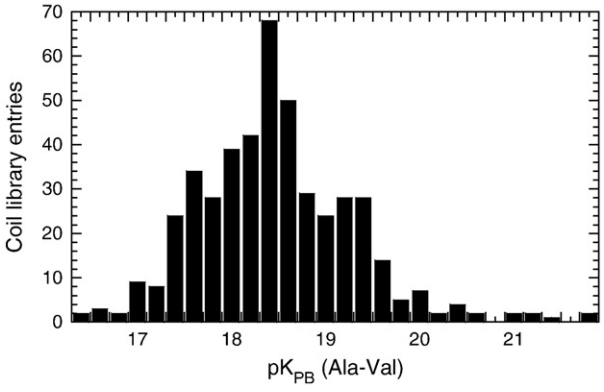

Fig. 1. Peptide acidities of N-acetyl-[Ala-Val]-N-methylamide conformers. The Poisson–Boltzmann (PB) electrostatic free energies were calculated for the central peptide anions formed from blocked peptides derived from the 458 Ala-Val segments found in the Protein Coil Library [45]. The CHARMM22 atomic charge and radius parameters [51] were modified to incorporate density functional theory-derived atomic charges for the peptide anion [7]. An internal dielectric value of 3 was applied, and an N-methylacetamide anion was used as internal reference of differential acidity. The experimental hydrogen exchange rate of N-acetyl-[Ala-Ala-Ala]-N-methylamide [37] was used to provide reference to an absolute pK scale.

influences the predicted conformer acidities can be assessed by analysis of the Protein Coil Library [Ala-Val] peptide conformations with the valine sidechain truncated to alanine. For each of the three χ_1 rotamers of the valine sidechain, the acidity of the central amide is closely correlated with that of the [Ala-Ala] peptide in the same backbone geometry (Fig. 2). However, conformers with the g^- sidechain rotamer, in which both methyl groups are oriented gauche to the backbone nitrogen, are predicted to have appreciably lower amide acidities (on average ~0.7 pH units). Throughout the range of amide acidities, differences in the sidechain χ_1 torsion angle give rise to variations in pK values spanning ~1 pH unit.

The average conformer exchange reactivity was calculated for each of the nonpolar N-acetyl-[X-Ala]-N-methylamide and N-acetyl-[Ala-Y]-N-methylamide conformers (Fig. 3). The Poisson–Boltzmann analysis of the Protein Coil Library-derived conformational ensemble for the nonpolar residues predicts the experimental differential log rate constants $\Delta\log k_{OH^-}$ for hydrogen exchange to within an rmsd value of 0.11 and a correlation coefficient $r = 0.91$. However, despite the fact that the hydrogen exchange prediction for each peptide is based on a different set of crystallographic conformers with amide acidities spanning nearly a million-fold range, the experimental exchange rates are predicted with an average error of 30% ($10^{0.11}$). Although the nonpolar [Ala-Y] peptides exhibit a substantially larger range of experimental $\Delta\log k_{OH^-}$ values than do the nonpolar [X-Ala] peptides, the exchange rate predictions are of comparable precision for both. Since the slope of the correlation between the observed and predicted $\Delta\log k_{OH^-}$ values varies inversely with the assumed internal dielectric value, even for simple peptides [36], the correlation among the nonpolar [X-Ala] and [Ala-Y] peptides indicates that dielectric shielding in the timeframe of the peptide anion lifetime is well approximated by an internal dielectric value of 3. Thus, despite the enhanced conformational dynamics of small model peptides, conformational reorganization does not appear to provide a substantial contribution to the acidity of these peptides. The issue of conformational reorganization is examined in more detail during the analysis of hydrogen exchange for polar residues, considered below.

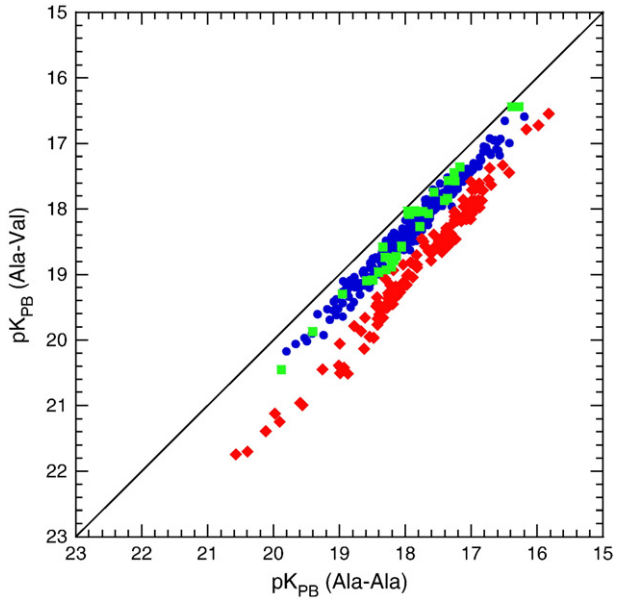

Fig. 2. Relative contributions of sidechain and mainchain interactions determining the peptide acidities of N-acetyl-[Ala-Val]-N-methylamide conformers. For each of the N-acetyl-[Ala-Val]-N-methylamide conformers analyzed in Fig. 1, the methyl groups were truncated to form an [Ala-Ala] conformer, and the electrostatic free energy was calculated. The corresponding pairs of amide pK values are denoted by their χ_1 sidechain rotamer (g^- as red diamonds, g^+ as green squares and t as blue circles).

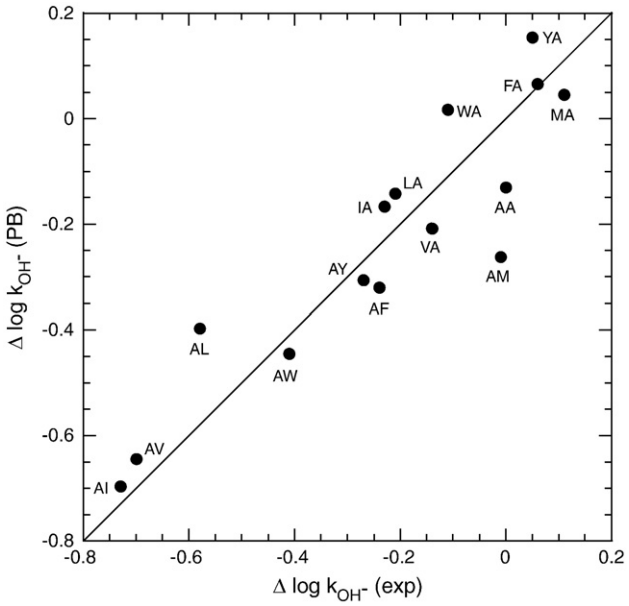

Fig. 3. Predicted and observed nonpolar sidechain-dependent differences in the hydroxide-catalyzed log rate constants for model peptides. Poisson–Boltzmann electrostatic free energies were calculated for the N-acetyl-[X-Ala]-N-methylamide conformers and N-acetyl-[Ala-Y]-N-methylamide conformers derived from the Protein Coil Library [45]. Hydrogen exchange rate constants were predicted from the ensemble averaging of the conformer exchange reactivities and were then compared to the standard experimental sidechain-dependent hydrogen exchange correction factors [37].

3.3. Deviations from additivity in the nonpolar sidechain correction factors for hydrogen exchange

The standard experimental values for the sidechain-dependent differential exchange rates were derived from measurements on N-acetyl-[X]-N-methylamide dipeptides [37]. These values are used to predict hydrogen exchange rates in conformationally unstructured peptides by summing together the correction factors for both the sidechain preceding the amide and the sidechain following that amide. This assumption of additivity for the individual sidechain-dependent hydrogen exchange correction factors has its conceptual justification in the isolated residue hypothesis of Flory, developed in his classic analysis of the statistical mechanics of random coil polymers [61]. In that paradigm, the conformational distribution of each residue is assumed to be independent of the conformational distribution of any other residue in the chain.

Direct evidence for violation of the isolated residue hypothesis [61] was reported by Penkett et al. [62] who observed that the backbone Φ torsion angle of a given residue, as assessed on the basis of the $^3J_{HN\alpha}$ NMR scalar coupling constant, is dependent on whether the preceding residue has a β-branched or an aromatic sidechain. The presence of a bulky nonpolar sidechain on the preceding residue was found to increase the population of conformers having extended (β-like) mainchain torsion angles. Studies of coil libraries drawn from high resolution protein X-ray structures have found nearest-neighbor effects in the backbone torsion angle preferences [63,64].

Avbelj and Baldwin [35] have reported that the calculated electrostatic solvation free energy of a backbone amide is dependent upon whether a bulky nonpolar sidechain is present on the preceding residue. The present calculations provide a further opportunity to examine the degree to which the assumption of additivity in the standard sidechain-dependent hydrogen exchange correction factors [37] may give rise to systematic errors in the predicted exchange rates for conformationally disordered peptides.

Evidence for non-additivity of the sidechain-dependent hydrogen exchange correction factors can be directly examined by comparing

the peptide acidity predictions of N-acetyl-[X-Ala]-N-methylamides and N-acetyl-[Ala-Y]-N-methylamides to those of the other N-acetyl-[X-Y]-N-methylamides. Deviations from additivity for these calculations are unlikely to arise from the continuum dielectric algorithm itself. Although the nonlinear form of the Poisson–Boltzmann equation was used for these calculations, we have previously reported [6,22] that the linear form yields highly similar results for such peptide acidity studies. Instead, a substantial degree of non-additivity in these calculations should only arise due to deviations from the isolated residue hypothesis [61] via the resultant variations among the conformational distributions for each of the N-acetyl-[X-Y]-N-methylamides.

If the conformer distributions from the Protein Coil Library [45] perfectly conformed to the isolated residue hypothesis, then the differential hydrogen exchange rates predicted for each N-acetyl-[X-Y]-N-methylamide might be expected to be precisely determined by the sum of the $\Delta\log k_{OH^-}$ values for the corresponding N-acetyl-[X-Ala]-N-methylamide and N-acetyl-[Ala-Y]-N-methylamide (Fig. 3). However, the predictions assuming additivity in the calculated nonpolar sidechain-dependent hydrogen exchange correction factors deviate from the N-acetyl-[X-Y]-N-methylamide calculations with an rmsd of 0.14 and a correlation coefficient $r = 0.78$ (Fig. 4). This correlation is substantially worse than that for the predictions of the experimental nonpolar sidechain-dependent hydrogen exchange correction factors, despite the fact that the calculations illustrated in Fig. 3 have several additional sources of uncertainty.

The calculations for the N-acetyl-[X-Y]-N-methylamides (Fig. 4) test only the internal consistency of the assumption that the peptide conformational distributions reflect the isolated residue hypothesis. In contrast, the quality of the predictions for the experimental nonpolar sidechain-dependent hydrogen exchange correction factors in Fig. 3 rely upon the physical accuracy of both the continuum dielectric paradigm and the specific electrostatic parameters applied. Furthermore, the normal Eigen acid/base analysis relating thermodynamic acidity to the hydrogen exchange kinetics is a useful approximation rather than a formally exact result. In addition, discrepancies between the predicted and experimental sidechain-dependent hydrogen exchange correction factors must also reflect the measurement errors. Despite each of these additional sources of uncertainty, the prediction of the experimental nonpolar sidechain-dependent hydrogen exchange correction factors is appreciably more precise than the deviations that arise in the corresponding calculations under the assumption of the additivity of these hydrogen exchange correction factors.

The magnitude of the deviations that are predicted to arise from the assumption of additivity for sidechain-dependent hydrogen exchange correction factors appear to be consistent with the limited set of direct experimental comparisons previously reported. In testing the additivity principle for these correction factors, Englander and colleagues [37] presented experimental exchange data from two unblocked hexapeptides and a pentapeptide. Among the 10 amides for which the base-catalyzed data were reported, three of the amides yielded experimental rates that deviated by ~0.5 log units from the rate predicted by addition of the sidechain-dependent correction factors.

3.4. Conformational reorganization in the amide hydrogen exchange predictions for polar sidechains

In contrast to the $\Delta\log k_{OH^-}$ predictions for the nonpolar residues discussed above, the analogous calculations for the Asn and Gln sidechains predicted amide acidities that were appreciably less than the experimentally determined values (open symbols in Fig. 5). The analysis of the effects of nonpolar sidechains on amide exchange utilized the assumption that the lifetime of the peptide anion is sufficiently short so that the contribution to dielectric shielding arising from conformational reorganization is negligible. Substantial conformational reorganization for the nonpolar sidechains generally involves rotamer transitions around the sp^3–sp^3 bonds. NMR relaxation analysis indicates that such unhindered sidechain rotamer transitions in proteins generally occur in the timeframe of hundreds of picoseconds to nanoseconds [65,66]. Since such rotamer lifetimes are

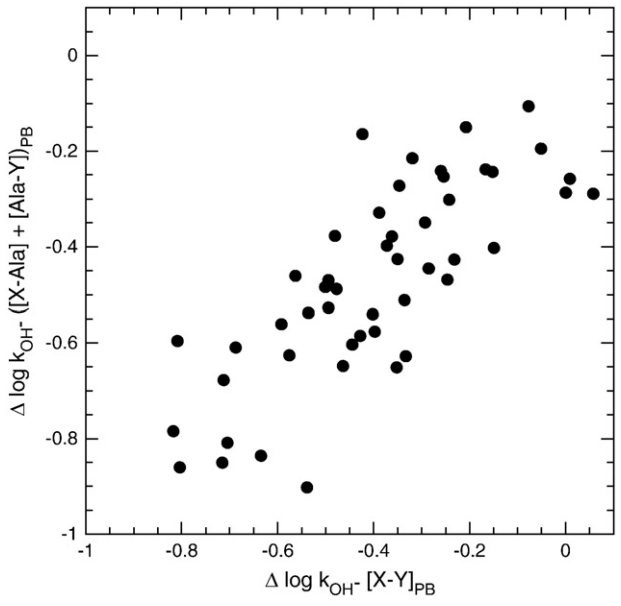

Fig. 4. Additivity for nonpolar sidechain-dependent differences in the hydroxide-catalyzed log rate constants in model peptides. Electrostatic free energies were used to predict the exchange reactivities for the N-acetyl-[X-Y]-N-methylamide conformers derived from the Protein Coil Library [45], excluding the Ala-containing peptides given in Fig. 3. These predicted rate constants, normalized to the alanine peptide reference, were compared to the sum of the analogous differential rate constants for the N-acetyl-[X-Ala]-N-methylamide and the N-acetyl-[Ala-Y]-N-methylamide plotted in Fig. 3.

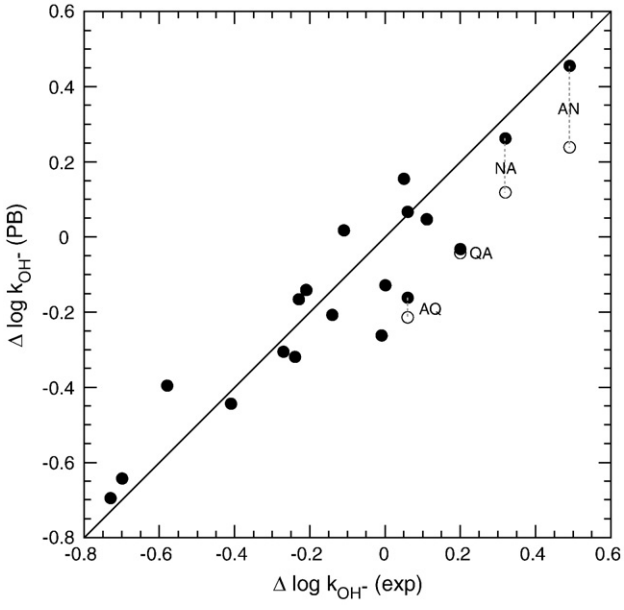

Fig. 5. The effect of conformational reorganization within the individual sidechain rotamer states for Asp (χ_1) and Gln (χ_1 and χ_2). Electrostatic free energies were calculated for the [Asp-Ala], [Ala-Asp], [Gln-Ala] and [Ala-Gln] methylamide conformers derived from the Protein Coil Library [45]. Hydrogen exchange rate constants were predicted from the ensemble averaging of these conformer exchange reactivities with (●) and (○) without allowance for conformational reorganization of the peptide anions within each sidechain rotamer state. The other data are displayed as given in Fig. 3.

substantially longer than that anticipated for the peptide anion (~10 ps [6,7,17]), these rotamer transitions are not expected to give rise to significant dielectric shielding of this anion.

Under the assumption of negligible conformational reorganization, each molecule that undergoes the ionization of a backbone amide maintains the same conformation from the time of the initial removal of the proton until the peptide anion is quenched by a neutral water molecule. However, if significant conformational reorganization can occur before the peptide anion is quenched, then the anion formed from a given initial conformation will be quenched from a range of conformations. More importantly, due to the altered electrostatic interactions, the Boltzmann weighting among those peptide anion conformations will generally differ from the Boltzmann weighting among the corresponding neutral peptide conformations. The fact that this effect appears to be modest and often negligible for peptide ionizations largely explains the relative simplicity of the dielectric shielding analysis of hydrogen exchange, as compared to the corresponding analysis required for the long-lived (μs–ms) protein sidechain ionizations.

Relative to the comparatively slow rotamer transitions at sp^3–sp^3 hybridized bonds, the sp^3–sp^2 hybridization of the carboxamide sidechain results in more rapid dihedral angle transitions due to the lower intrinsic torsional potential barrier, which quantum mechanical analysis indicates is only 0.15 kcal/mol for acetamide [67]. As a result, within each χ_1 rotamer state of Asn, extensive sampling of the χ_2 torsion angle can potentially occur during the peptide anion lifetime. Given the large dipole of the sidechain carboxamide group, such a bond rotation can substantially alter the degree of stabilization provided for the peptide anion.

Calculations were conducted to estimate the magnitude of the shielding effect from conformational reorganization of the Asn sidechain by assuming rapid averaging around the χ_2 torsion angle. The strength of the electrostatic interaction between the carboxamide group and the peptide anion was estimated for each conformer by subtracting the electrostatic free energy for the [Ala-Ala] peptide formed by truncating the carboxamide group. By assumption in our analysis, the conformational distribution from the Protein Coil Library represents the Boltzmann-weighted distribution for the neutral residue state. Upon deprotonation of the peptide unit, the statistical weighting of this distribution will shift according to the conformer-dependent strength of the electrostatic interaction between the carboxamide group and the peptide anion. The differences in energy among all of the conformer-dependent electrostatic interactions within a given χ_1 rotamer state were used to assign a Boltzmann factor weighting to each conformer within that χ_1 rotamer state. The analogous averaging was applied over the χ_3 torsion angle of the Gln sidechains for each of the χ_1 and χ_2 rotamer states.

Application of the carboxamide rotation correction for each χ_1 rotamer state of the [Ala-Asn] and [Asn-Ala] peptides and for each χ_1 and χ_2 rotamer state for the [Ala-Gln] and [Gln-Ala] peptides yielded the $\Delta\log k_{OH^-}$ values indicated by closed symbols in Fig. 5. For the Asn peptides, this correction for conformational reorganization brings the predicted peptide acidity fully in line with the experimental results. A smaller correction is predicted for the Gln sidechain, reflecting the larger average distance between the backbone nitrogen and the sidechain carboxamide. When this analysis of the Asn and Gln sidechains is combined with the predictions for the nonpolar sidechains, the overall rmsd with respect to the experimental values is 0.12 log units, with a correlation coefficient $r = 0.93$.

As we have previously discussed [7], the assumption of negligible conformational reorganization can be too stringent for the β-hydroxy amino acid sidechains. It is the reorientation of the hydrogen atoms in water that primarily gives rise to the dominant dielectric shielding contribution from the solvent phase. In the absence of intramolecular hydrogen bond interactions, a reasonable assumption is that the analogous rotation of an unrestrained hydroxyl hydrogen in a serine or threonine sidechain occurs in a similar timeframe. Unfortunately, in contrast to the carboxamide sidechains, there are comparatively few experimental data that can provide direct insight into the Boltzmann-weighted distribution of hydroxyl hydrogen atom orientations for any given heavy atom peptide conformation.

Particularly for serine or threonine hydroxyls in either a gauche$^+$ or gauche$^-$ χ_1 rotamer, the positioning of the hydroxyl hydrogen strongly affects the predicted electrostatic potential at the intraresidue backbone nitrogen. Given that the exchange rates for serine- and threonine-containing model peptides are similar to those of the alanine reference [37], direct interaction between the sidechain hydroxyl and the peptide anion peptide must not substantially perturb the hydrogen exchange reaction. Consistent with that observation, we have proposed [7] that peptide acidity analysis for a serine or threonine residue having a gauche χ_1 rotamer should assume that the dielectric shielding of the sidechain hydroxyl is equivalent to that of the equivalent volume of water. In such cases, the serine sidechain is computationally truncated to alanine, and threonine is transformed into α-aminobutyrate.

3.5. Ensemble-averaged amide hydrogen exchange predictions for charged sidechains

The Poisson–Boltzmann calculations of peptide acidities given above were all carried out at 0.15 M ionic strength, so as to mimic physiological conditions. In contrast, the hydrogen exchange experiments used to derive the standard sidechain-dependent correction factors were carried out at 0.5 M ionic strength, so as to more strongly suppress the effects of electrostatic interactions [37]. Englander and colleagues [37] noted that raising the ionic strength to 0.5 M decreased the base-catalyzed exchange rates for the uncharged sidechains by only about 7%. Consistent with that observation, our continuum dielectric calculations predicted negligible variations in the $\Delta\log k_{OH^-}$ values upon a change from 0.15 M to 0.5 M ionic strength for these residue types.

A change from 0.15 M to 0.5 M ionic strength gives rise to a modest but significant shift in the $\Delta\log k_{OH^-}$ values for the charged sidechains. In the case of the Lys, Arg and Glu peptides, accounting for the higher ionic strength of the experimental measurements yields a reasonably satisfactory match between the experimental and predicted exchange rates (Fig. 6). The experimental log exchange rate data for the nonpolar, Asn, Gln, Lys, Arg and Glu sidechains were predicted to an rmsd value of 0.16 and a correlation coefficient $r = 0.88$.

The predicted hydrogen exchange rate derived from the calculated peptide acidities for the Asp conformers is significantly lower than the experimental result, even after the elevated ionic strength of the hydrogen exchange measurements is taken into account. These deviations strongly suggest that the present calculations overestimate the effective strength of the electrostatic interaction between the peptide anion and the negatively charged Asp sidechain. Insight into these interactions can be gained from consideration of the distribution of conformer acidities as a function of sidechain rotamer state. When the [Ala-Asp] peptide conformers and the [Ala-Ala] peptide conformers generated by truncation of the carboxylate were compared (Fig. 7), both gauche χ_1 rotamer states yielded sidechain conformation-dependent variations in peptide acidities that were substantially larger than those obtained from the analogous predictions for the [Ala-Val] peptide conformers (Fig. 2). This effect is particularly marked for the g^+ rotamer state in which a substantial proportion of conformers have a carboxylate oxygen positioned close to the peptide nitrogen. In contrast, the [Ala-Asp] peptide conformers in the trans χ_1 rotamer state yield peptide conformer acidities that tightly correlate with the electrostatic interactions of the backbone, although the predictions are uniformly shifted to lower acidities, due to the long range interaction between the peptide anion and the trans carboxylate.

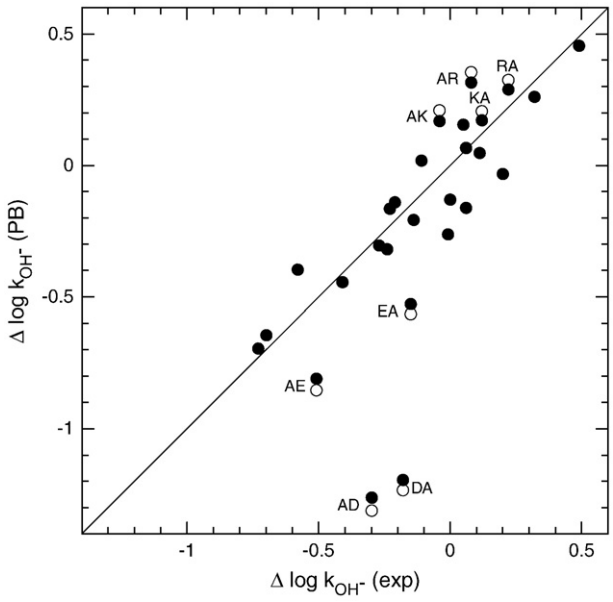

Fig. 6. The effect of ionic strength on the predicted hydrogen exchange rates for the charged Lys, Arg, Asp and Glu sidechains. Electrostatic free energies were calculated for the peptide conformers derived from the Protein Coil Library [45]. Hydrogen exchange rate constants were predicted from the ensemble averaging of the Lys, Arg, Asp and Glu conformer exchange reactivities for 0.5 M (●) and 0.15 M (○) ionic strength. The other data are displayed as given in Fig. 5.

Application of a carboxylate rotation correction to each χ_1 rotamer state, following the protocol described for the Asn sidechain, assigns a Boltzmann weighting to each of the [Ala-Asp] conformers illustrated in Fig. 7. This modeling of conformational reorganization strongly attenuates the contribution of the weakly acidic peptide conformers to the population estimate of the observed hydrogen exchange rate. On the other hand, comparatively little change in statistical weighting occurs among the more highly acidic conformers that dominate the observed hydrogen exchange. In contrast to the Asn sidechain, in which the carboxamide dipole can reorient to generate a favorable electrostatic interaction with the peptide anion, the smaller rotamer state correction predicted for the Asp sidechain primarily reflects the fact that the negatively charged carboxylate in a given χ_1 rotamer state has a restricted ability to minimize the unfavorable interactions with the peptide anion.

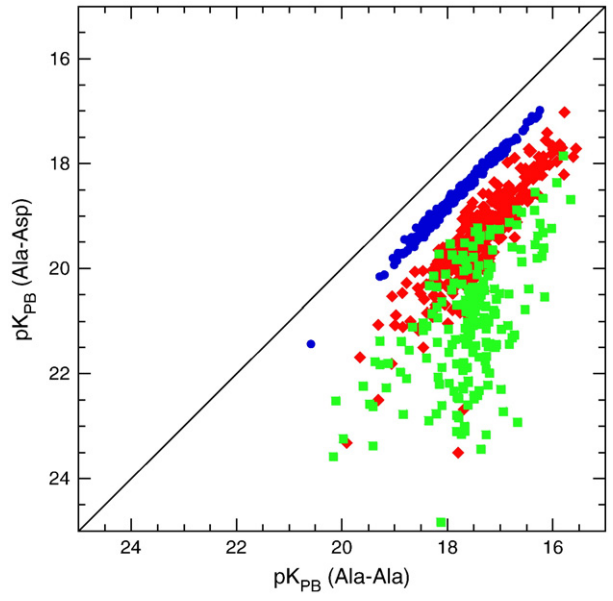

Fig. 7. The relative contributions of sidechain and mainchain interactions in determining the peptide acidities of N-acetyl-[Ala-Asp]-N-methylamide conformers. For each N-acetyl-[Ala-Asp]-N-methylamide, the carboxylate group was truncated to form an [Ala-Ala] conformer, and the electrostatic free energy was then calculated. The corresponding pairs of amide pK values are denoted by their χ_1 sidechain rotamer (g^- as red diamonds, g^+ as green squares and t as blue circles).

In the present analysis, the amide acidities for the Asp peptides are significantly underestimated. In marked contrast to each of the other residue types, our previous continuum dielectric studies of protein hydrogen exchange have reported the underestimation of exchange rates for Asp residues when the sidechain carboxylate is oriented gauche to the backbone nitrogen in the analysis of both single X-ray crystallographic structures [6,7] and molecular dynamics-derived ensembles [22].

The disparity between the predicted and observed hydrogen exchange rates for the Asp residues may reflect inadequacies in the continuum solvent representation of dielectric shielding for short-range intense electrostatic interactions. Alternately, given the comparatively strong unfavorable interactions between the Asp carboxylate and the peptide anion, rapid reorientation of the peptide backbone in response to peptide ionization may be facilitated. The (ϕ,ψ) torsion angle transitions between the helical and extended conformations have been predicted to occur in the timeframe of 200 ps in small model peptides [68,69], and thus should be too slow to provide efficient dielectric shielding for the amide anion. On the other hand, transitions between the extended and polyproline II conformations have been predicted to occur in the 10 ps timeframe [68], similar to the lifetime of the peptide anion.

3.6. Chemical induction in peptide hydrogen exchange

The nonpolarizable CHARM22 [51] electrostatic parameter set ascribes the same fixed charge and radius parameters to every residue type considered herein for each of the mainchain N, H, C and O atoms. This assumed uniformity in the backbone charge distribution implies that no sidechain-dependent covalent shift of electron density can be modeled that would differentially stabilize the peptide anion. However, despite having excluded a representation of chemical induction effects within the protein backbone, the experimental $\Delta\log\ k_{OH^-}$ values were reasonably accurately predicted by the CHARMM22 electrostatic parameter set for all of the residue types illustrated in Fig. 6, excepting Asp. In this context, it may be noted that the AMBER parm99 [70] and AMBER ff03 [71] nonpolarizable force fields utilize electrostatic parameter sets in which the partial charges of the mainchain atoms vary as a function of the sidechain type. The poor performance in prediction of peptide acidities provided by the AMBER electrostatic parameter sets suggests that these force fields markedly overestimate the magnitude of the chemical induction effects that are being implicitly modeled [7].

The direct electrostatic interaction between the peptide anion and the carboxylate sidechains of Asp estimated in the previous section overpredicts the decrease in hydroxide-catalyzed exchange rates that is observed to occur for these peptides. Any significant electron-donating covalent chemical induction effect from the sidechain carboxylate will serve to destabilize the peptide anion and thus exacerbate the disparity between the predicted and observed exchange behavior.

In contrast, the Ser, Thr, Cys and His^+ intraresidue sidechains all accelerate hydroxide-catalyzed peptide hydrogen exchange [37], consistent with an electron-withdrawing effect from the substituent. However, the challenges facing an adequate modeling of the electrostatic potential for these sidechains complicate the deconvolution of an additional contribution to peptide acidity arising from chemical induction. As discussed above for the β-hydroxyl bearing

sidechains, the predicted electrostatic potential at the peptide nitrogen is acutely sensitive to the assumed orientation of the ill-determined hydroxyl hydrogen. In the case of the histidine sidechains, the protein X-ray coordinates generally do not unambiguously distinguish between the positively charged state and either of the two neutral tautomers, thus complicating the interpretation of continuum dielectric calculations based on this structural library. Our recent demonstration [72] that the neutral histidine sidechain can serve as an efficient general base catalyst of peptide hydrogen exchange in a protein active site near neutral pH illustrates an additional complexity for the continuum dielectric analysis of exchange at histidine residues.

Since the contribution from chemical induction is largely independent of conformation, the standard peptide $\Delta\log k_{OH^-}$ values, normalized to the Ala sidechain, can be used to predict the upper limits for any chemical induction correction for the β-hydroxy, Cys and His^+ sidechains. Since the range of hydrogen exchange rates observed in protein measurements greatly exceeds the range of these peptide correction factors, the β-hydroxy, Cys and His residues can still be used to provide useful constraints upon the accuracy of any protocol developed for quantitative prediction.

4. Conclusion

Using the Protein Coil Library of Rose and colleagues [45] as a representation of the Boltzmann-weighted distribution for conformationally unstructured peptides, the hydroxide-catalyzed exchange rates are accurately predictable for the majority of the sidechain types utilizing continuum dielectric methods based on the assumptions of atom-centered fixed partial charges and uniform volume polarizabilities. Although both of these assumptions regarding the representation of electrostatics are only approximate, it remains unclear whether the residual inaccuracies in the predictions of hydrogen exchange for either proteins or model peptides primarily reflect the errors in the modeling of the Boltzmann conformational distribution or rather the inadequacies in the electrostatic modeling used to analyze those conformations. Future studies must pursue both of these avenues for improved predictive capability. However, as recently observed by Senn and Thiel [73], despite many years of intense research effort, there are as yet no generally established polarizable biomolecular force fields. Fortunately, the present studies further demonstrate that, in the context of dielectric shielding without substantial conformational reorganization, the classic paradigm of uniform volume polarizability is strikingly robust.

The rmsd of 0.11 obtained for prediction of the $\Delta\log k_{OH^-}$ values for the nonpolar model peptides is far more precise than the current optimal performance for the analogous predictions of hydrogen exchange for static solvent-exposed amides in natively folded proteins [7,22]. On the other hand, the correlation coefficient $r = 0.88$ with which the majority of sidechain-dependent hydrogen exchange rate effects can be predicted is similar to what has been obtained in the protein hydrogen exchange predictions, reflecting the much narrower range of experimental rate constants that were observed in the model peptide studies [37].

The modeling of rapid conformational relaxation around the sp^3–sp^2 bond in the sidechains of the Asn and Gln residues yields a significant improvement in the corresponding hydrogen exchange predictions. Ambiguities regarding the orientation of hydroxyl hydrogens and chemical induction effects for the Ser, Thr and Cys residues as well as possible ambiguities regarding the protonation states of histidines limit the predictability of these residue types, although these uncertainties are modest as compared to the range of rates observed in protein exchange studies. The prediction of hydrogen exchange for Asp residues remains comparatively problematic.

Our recent predictions of hydrogen exchange for model representations of the native state conformational ensemble of ubiquitin [22] demonstrated the acute sensitivity with which electrostatic analysis can identify deviations from the correct Boltzmann weighting of the conformational ensemble. The present results offer significant support to the interpretation that properly curated libraries of conformations drawn from high resolution X-ray structures can provide useful representations for the distribution of peptides and proteins in the conformationally unstructured state. The analysis of the nonpolar peptides demonstrates that hydrogen exchange is sensitive to differences in the peptide-specific conformational distributions which give rise to non-additivity for the standard sidechain-dependent correction factors [37].

References

[1] A. Hvidt, K. Linderstrøm-Lang, Exchange of hydrogen atoms in insulin with deuterium atoms in aqueous solutions, Biochim. Biophys. Acta 14 (1954) 574–575.
[2] A. Berger, K. Linderstrøm-Lang, Deuterium exchange of poly-DL-alanine in aqueous solution, Arch. Biochem. Biophys. 69 (1957) 106–118.
[3] S.O. Nielsen, W.P. Bryan, K. Mikkelsen, Hydrogen–deuterium exchange of small peptides in aqueous solution, Biochim. Biophys. Acta 42 (1960) 550–552.
[4] A. Hvidt, S.O. Nielsen, Hydrogen exchange in proteins, Advances in Protein Chem. 21 (1966) 287–386.
[5] Y.W. Bai, J.S. Milne, L. Mayne, S.W. Englander, Protein stability parameters measured by hydrogen exchange, Proteins: Struct., Funct., Genet. 20 (1994) 4–14.
[6] J.S. Anderson, G. Hernández, D.M. LeMaster, A billion-fold range in acidity for the solvent-exposed amides of *Pyrococcus furiosus* rubredoxin, Biochemistry 47 (2008) 6178–6188.
[7] G. Hernández, J.S. Anderson, D.M. LeMaster, Polarization and polarizability assessed by protein amide acidity, Biochemistry 48 (2009) 6482–6494.
[8] M. Schaefer, M. Karplus, A comprehensive analytical treatment of continuum electrostatics, J. Phys. Chem. 100 (1996) 1578–1599.
[9] J. Antosiewicz, J.A. McCammon, M.K. Gilson, Prediction of pH dependent properties of proteins, J. Mol. Biol. 238 (1994) 415–436.
[10] J. Antosiewicz, J.A. McCammon, M.K. Gilson, The determinants of pKas in proteins, Biochemistry 35 (1996) 7819–7833.
[11] E. Demchuk, R.C. Wade, Improving the continuum dielectric approach to calculating pKa's of ionizable groups in proteins, J. Phys. Chem. 100 (1996) 17373–17387.
[12] R.E. Georgescu, E.G. Alexov, M.R. Gunner, Combining conformational flexibility and continuum electrostatics for calculating pKas in proteins, Biophys. J. 83 (2002) 1731–1748.
[13] M.S. Wisz, H.W. Hellinga, An empirical model for electrostatic interactions in proteins incorporating multiple geometry-dependent dielectric constants, Proteins 51 (2003) 360–377.
[14] Y. Song, J. Mao, M.R. Gunner, MCCE2: improving protein pKa calculations with extensive side chain rotamer sampling, J. Comput. Chem. 30 (2009) 2231–2247.
[15] T. Simonson, D. Perahia, Internal and interfacial dielectric properties of cytochrome c from molecular dynamics in aqueous solution, Proc. Natl. Acad. Sci. USA 92 (1995) 1082–1086.
[16] R.A. Marcus, Chemical and electrochemical electron-transfer theory, Annu. Rev. Phys. Chem. 15 (1964) 155–196.
[17] D.M. LeMaster, J.S. Anderson, G. Hernández, Spatial distribution of dielectric shielding in the interior of *Pyrococcus furiosus* rubredoxin as sampled in the subnanosecond timeframe by hydrogen exchange, Biophys. Chem. 129 (2007) 43–48.
[18] R.S. Molday, R.G. Kallen, Substituent effects on amide hydrogen exchange rates in aqueous solution, J. Am. Chem. Soc. 94 (1972) 6739–6745.
[19] W.H. Wang, C.C. Cheng, General base catalyzed proton exchange in amides, Bull. Chem. Soc. Jpn. 67 (1994) 1054–1057.
[20] M. Eigen, Proton transfer, acid–base catalysis, and enzymatic hydrolysis. (I) Elementary processes, Angew. Chem. Int. Ed. 3 (1964) 1–19.
[21] E.L. Mertz, L.I. Krishtalik, Low dielectric response in enzyme active site, Proc. Natl. Acad. Sci. USA 97 (2000) 2081–2086.
[22] D.M. LeMaster, J.S. Anderson, G. Hernández, Peptide conformer acidity analysis of protein flexibility monitored by hydrogen exchange, Biochemistry 48 (2009) 9256–9265.
[23] B. Richter, J. Gsponer, P. Varnai, X. Salvatella, M. Vendruscolo, The MUMO (minimal under-restraining minimal over-restraining) method for the determination of native state ensembles of proteins, J. Biomol. NMR 37 (2007) 117–135.
[24] O.F. Lange, N.A. Lakomek, C. Fares, G.F. Schroder, K.F.A. Walter, S. Becker, J. Meiler, H. Grubmuller, C. Griesinger, B.L. deGroot, Recognition dynamics up to microseconds revealed from an RDC-derived ubiquitin ensemble in solution, Science 320 (2008) 1471–1475.
[25] E. Mehler, F. Guarnieri, A self-consistent, microenvironment modulated screened Coulomb potential approximation to calculate pH-dependent electrostatic effects in proteins, Biophys. J. 77 (1999) 3–22.
[26] T. Simonson, J. Carlsson, D.A. Case, Proton binding to proteins: pKa calculations with explicit and implicit solvent models, J. Am. Chem. Soc. 126 (2004) 4167–4180.
[27] J.H. Jensen, H. Li, A.D. Robertson, P.A. Molina, Prediction and rationalization of protein pK(a) values using QM and QM/MM methods, J. Phys. Chem. A 109 (2005) 6634–6643.

[28] H. Li, A.D. Robertson, J.H. Jensen, Very fast empirical prediction and rationalization of protein pKa values, Prot. Struct. Funct. Bioinform. 61 (2005) 704–721.
[29] J. Khandogin, C.L. Brooks III, Toward the accurate first-principles prediction of ionization equilibria in proteins, Biochemistry 45 (2006) 9363–9373.
[30] P. Barth, T. Alber, P.B. Harbury, Accurate, conformation-dependent predictions of solvent effects on protein ionization constants, Proc. Natl. Acad. Sci U. S. A 104 (2007) 4898–4903.
[31] V.Z. Spassov, L. Yan, A fast and accurate computational approach to protein ionization, Prot. Sci. 17 (2008) 1955–1970.
[32] D.C. Bas, D.M. Rogers, J.H. Jensen, Very fast prediction and rationalization of pK(a) values for protein–ligand complexes, Proteins Struct. Funct. Bioinform. 73 (2008) 765–783.
[33] M. Sheinblatt, Determination of an acidity scale for peptide hydrogens from nuclear magnetic resonance kinetic studies, J. Am. Chem. Soc. 92 (1970) 2505–2509.
[34] F. Fogolari, G. Esposito, P. Viglino, J.M. Briggs, J.A. McCammon, pKa shift effects on backbone amide base-catalyzed hydrogen exchange rates in peptides, J. Am. Chem. Soc. 120 (1998) 3735–3738.
[35] F. Avbelj, R.L. Baldwin, Origin of the neighboring residue effect on peptide backbone conformation, Proc. Natl. Acad. Sci. USA 101 (2004) 10967–10972.
[36] J.S. Anderson, G. Hernández, D.M. LeMaster, Backbone conformational dependence of peptide acidity, Biophys. Chem. 141 (2009) 124–130.
[37] Y.W. Bai, J.S. Milne, L. Mayne, S.W. Englander, Primary structure effects on peptide group hydrogen-exchange, Proteins: Struct., Funct., Genet. 17 (1993) 75–86.
[38] D. Sitkoff, K.A. Sharp, B. Honig, Accurate calculation of hydration free energies using macroscopic solvent models, J. Phys. Chem. 98 (1994) 1978–1988.
[39] J. Makowska, S. Rodziewicz-Motowidło, K. Bagińska, J.A. Vila, A. Liwo, L. Chmurzyński, H.A. Scheraga, Polyproline II conformation is one of many local conformational states and is not an overall conformation of unfolded peptides and proteins, Proc. Natl. Acad. Sci. USA 103 (2006) 1744–1749.
[40] K. Chen, Z. Liu, C. Zhou, W.C. Bracken, N.R. Kallenbach, Spin relaxation enhancement confirms dominance of extended conformations in short alanine peptides, Angew. Chem. Int. Ed. 46 (2007) 9036–9039.
[41] J. Graf, P.H. Nguyen, G. Stock, H. Schwalbe, Structure and dynamics of the homologous series of alanine peptides: a joint molecular dynamics/NMR study, J. Am. Chem. Soc. 129 (2007) 1179–1189.
[42] L. Wickstrom, A. Okur, C. Simmerling, Evaluating the performance of the ff99SB force field based on NMR scalar coupling data, Biophys. J. 97 (2009) 853–856.
[43] S. Pizzanelli, C. Forte, S. Monti, G. Zandomeneghi, A. Hagarman, T.J. Measey, R. Schweitzer-Stenner, Conformations of phenylalanine in the tripeptides AFA and GFG probed by combining MD simulations with NMR, FTIR, Polarized Raman, and VCD spectroscopy, J. Phys. Chem. B 114 (2010) 3965–3978.
[44] M. Tsai, Y.J. Xu, J.J. Dannenberg, Ramachandran revisited. DFT energy surfaces of diastereomeric trialanine peptides in the gas phase and aqueous solution, J. Phys. Chem. B 113 (2009) 309–318.
[45] N.C. Fitzkee, P.J. Fleming, G.D. Rose, The Protein Coil Library: a structural database of nonhelix, nonstrand fragments derived from the PDB, Prot. Struct. Funct. Bioinform. 58 (2005) 852–854.
[46] F. Avbelj, R.L. Baldwin, Limited validity of group additivity for the folding energetics of the peptide group, Prot. Struct. Funct. Bioinform. 63 (2006) 283–289.
[47] L.L. Perskie, T.O. Street, G.D. Rose, Structures, basins, and energies: a deconstruction of the Protein Coil Library, Prot. Sci. 17 (2008) 1151–1161.
[48] R.A. Laskowski, M.W. MacArthur, D.S. Moss, J.M. Thornton, PROCHECK: a program to check the stereochemical quality of protein structures, J. Appl. Cryst. 26 (1993) 283–291.
[49] J.M. Word, S.C. Lovell, J.S. Richardson, D.C. Richardson, Asparagine and glutamine: using hydrogen atom contacts in the choice of side-chain amide orientation, J. Mol. Biol. 285 (1999) 1733–1747.
[50] W. Rocchia, S. Sridharan, A. Nicholls, E. Alexov, A. Chiabrera, B. Honig, Rapid grid-based construction of the molecular surface and the use of induced surface charge to calculate reaction field energies: applications to the molecular systems and geometric objects, J. Comput. Chem. 23 (2002) 128–137.
[51] A.D. MacKerell Jr., D. Bashford, M. Bellott, R.L. Dunbrack Jr., J.D. Evanseck, M.J. Field, S. Fischer, J. Gao, H. Guo, S. Ha, D. Joseph-McCarthy, L. Kuchnir, K. Kuczera, F.T.K. Lau, C. Mattos, S. Michnick, T. Ngo, D.T. Nguyen, B. Prodhom, W.E. Reiher III, B. Roux, M. Schlenkrich, J.C. Smith, R. Stote, J. Straub, M. Watanabe, J. Wiorkiewicz-Kuczera, D. Yin, M. Karplus, All-atom empirical potential for molecular modeling and dynamics studies of proteins, J. Phys. Chem. B 102 (1998) 3586–3616.
[52] G.P. Connelly, Y.W. Bai, M.F. Jeng, S.W. Englander, Isotope effects in peptide group hydrogen-exchange, Proteins: Struct., Funct., Genet. 17 (1993) 87–92.
[53] Z. Luz, S. Meiboom, The activation energies of proton transfer reactions in water, J. Am. Chem. Soc. 86 (1964) 4768–4769.
[54] L.M. Tolbert, K.M. Solntsev, Excited-state proton transfer: from constrained systems to "super" photoacids to superfast proton transfer, Acc. Chem. Res. 35 (2002) 19–27.
[55] P. Leiderman, L. Genosar, D. Huppert, Excited-state proton transfer: indication of three steps in the dissociation and recombination process, J. Phys. Chem. A 109 (2005) 5965–5977.
[56] W.J. Ellison, K. Lamkaouchi, J.M. Moreau, Water: a dielectric reference, J. Molec. Liquids 68 (1996) 171–279.
[57] F.M. Richards, The interpretation of protein structures: total volume, group volume distributions and packing density, J. Mol. Biol. 82 (1974) 1–14.
[58] J. Tsai, R. Taylor, C. Chothia, M. Gerstein, The packing density in proteins: standard radii and volumes, J. Mol. Biol. 290 (1999) 253–266.
[59] J.S. Anderson, G. Hernandez, D.M. LeMaster, Conformational electrostatics in the stabilization of the peptide anion, Curr. Org. Chem. 14 (2010) 162–180.
[60] A.D. Becke, Density-functional thermochemistry III. The role of exact exchange, J. Chem. Phys. 98 (1993) 5648–5652.
[61] P.J. Flory, Statistical Mechanics of Chain Molecules, Wiley Interscience, New York, 1969.
[62] C.J. Penkett, C. Redfield, I. Dodd, J. Hubbard, D.L. McBay, D.E. Mossakowska, R.A.G. Smith, C.M. Dobson, L.J. Smith, NMR analysis of main-chain conformational preferences in an unfolded fibronectin-binding protein, J. Mol. Biol. 274 (1997) 152–159.
[63] O. Keskin, D. Yuret, A. Gursoy, M. Turkay, B. Erman, Relationships between amino acid sequences and backbone torsion angle preferences, Prot. Struct. Funct. Bioinform. 55 (2004) 992–998.
[64] A.K. Jha, A. Colubri, M.H. Zaman, S. Koide, T.R. Sosnick, K.F. Freed, Helix, sheet, and polyproline II frequencies and strong nearest neighbor effects in a restricted coil library, Biochemistry 44 (2005) 9691–9702.
[65] D.M. LeMaster, NMR relaxation order parameter analysis of the dynamics of protein sidechains, J. Am. Chem. Soc. 121 (1999) 1726–1742.
[66] N.R. Skrynnikov, O. Millet, L.E. Kay, Deuterium spin probes of side-chain dynamics in proteins. 2. Spectral density mapping and identification of nanosecond time-scale side-chain motions, J. Am. Chem. Soc. 124 (2002) 6449–6460.
[67] M.G. Darley, P.L.A. Popelier, Role of short-range electrostatics in torsional potentials, J. Phys. Chem. A 112 (2008) 12954–12965.
[68] Y. Mu, D.S. Kosov, G. Stock, Conformational dynamics of trialanine in water 2. Comparison of AMBER, CHARMM, GROMOS, and OPLS force fields to NMR and Infrared experiments, J. Phys. Chem B 107 (2003) 5064–5073.
[69] M.H. Zaman, M.Y. Shen, R.S. Berry, K.F. Freed, T.R. Sosnick, Investigations into sequence and conformational dependence of backbone entropy, inter-basin dynamics and the Flory isolated-pair hypothesis for peptides, J. Mol. Biol. 331 (2003) 693–711.
[70] T.E. Cheatham, P. Cieplak, P.A. Kollman, A modified version of the Cornell et al. force field with improved sugar pucker phases and helical repeat, J. Biomolec. Struct. Dyn. 16 (1999) 845–862.
[71] Y. Duan, C. Wu, S. Chowdhury, M.C. Lee, G.M. Xiong, W. Zhang, R. Yang, P. Cieplak, R. Lou, T. Lee, J. Caldwell, J.M. Wang, P. Kollman, A point-charge force field for molecular mechanics simulations of proteins based on condensed-phase quantum mechanical calculations, J. Comp. Chem. 24 (2003) 1999–2012.
[72] G. Hernández, J.S. Anderson, D.M. LeMaster, Electrostatic stabilization and general base catalysis in the active site of the human protein disulfide isomerase a domain monitored by hydrogen exchange, Chem. Bio. Chem. 9 (2008) 768–778.
[73] H.M. Senn, W. Thiel, QM/MM methods for biomolecular systems, Angew. Chem. Int. Ed. 48 (2009) 1198–1229.